EPJ manuscript No.
(will be inserted by the editor)

Magnetic and quantum entanglement properties of the distorted diamond chain model for azurite

Nerses Ananikian[1,2], Hrachya Lazaryan[1], and Mikayel Nalbandyan[1]

[1] A.I. Alikhanyan National Science Laboratory, Alikhanian Br. 2, 0036 Yerevan, Armenia
[2] Departamento de Ciencias Exatas, Universidade Federal de Lavras, CP 3037, 37200-000, Lavras- MG, Brazil

Received: date / Revised version: date

Abstract. We present the results of magnetic properties and entanglement of the distorted diamond chain model for azurite using pure quantum exchange interactions. The magnetic properties and concurrence as a measure of pairwise thermal entanglement have been studied by means of variational mean-field like treatment based on Gibbs-Bogoliubov inequality. Such a system can be considered as an approximation of the natural material azurite, $Cu_3(CO_3)_2(OH)_2$. For values of exchange parameters, which are taken from experimental results, we study the thermodynamic properties, such as azurite specific heat and magnetic susceptibility. We also have studied the thermal entanglement properties and magnetization plateau of the distorted diamond chain model for azurite.

1 Introduction

Copper oxide materials as low-dimensional magnetic systems are interesting subjects to investigate because of the new physics that can arise in low temperatures. The natural material azurite $Cu_3(CO_3)_2(OH)_2$ is the one of such copper oxide material which has been the subject of debates in recent years [1,2,3,4,6,7,8].

Moreover, azurite can be considered as one of the first experimental realizations of the 1D distorted ($J_1 \neq J_3$) diamond chain model (see Figure 1, for the detailed structure of azurite see for example [2]). It shows antiferromagnetic behavior at temperatures below Neel temperature 1.9 K [9]. Both the experimental analysis and theoretical modeling have been performed, but there is no clarity about exact values of the relative exchange interactions between azurite's copper ions [1,2,3,4,6,7,8]. On the other hand, there is significant evidence that the magnitude of the exchange interaction J_2 is the greatest one, forming dimers and monomers of Cu- ions [2,4,7]. In [2] an effective generalized spin-1/2 diamond chain model has been suggested with a dominant antiferromagnetic Cu-ions of the dimer coupling J_2, two antiferromagnetic Cu-ions of the dimer-monomer couplings J_1 and J_3, as well as a significant direct monomer- monomer of Cu-ions J_m exchange which explains a broad range of experiments on azurite and resolves the existing controversies.

The most noticeable feature is that there is a large magnetization plateau at 1/3 of the saturation magnetization [4], which extends from 11 to 30 T, when the magnetic field is applied in the perpendicular to the chain axis. Such 1/3 plateau is usually associated with classical up-up-down (uud) type of spin arrangement (or with a quantum state which has a classical analogue), while the 1/3 plateau of azurite is proposed to be of fundamentally different, $00u$ type, where the dominant J_2 coupling ensures that the two "dimer" spins on the Cu_2 sites (see Figure 1) are in a singlet state, while the third "monomer" (Cu_1) spin is completely polarized by the magnetic field. This state is based on the presence of a singlet and is a pure quantum nature without a classical analogue. Therefore azurite is the first successful candidate for describing a 1/3 quantum plateau state [10,11]. Another characteristic feature is that there is almost a direct transition from the plateau of saturation, which may be an interpretation as a remnant of the so-called localized magnon-members present in a perfect chain of diamond [12,13].

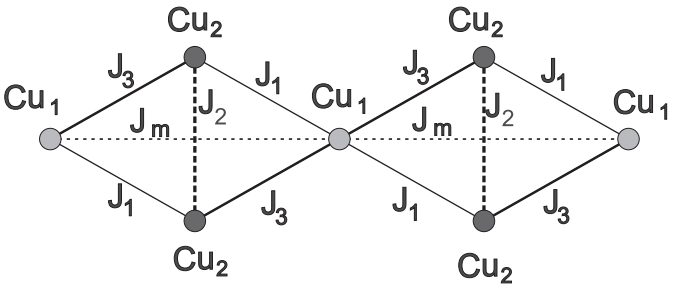

Fig. 1. Distorted diamond chain.

The phenomenon of magnetization plateau has been studied during the past decade both experimentally and theoretically. The plateau may exist in the magnetization curves of quantum spin systems in the case of a strong magnetic external field at low temperatures. Magnetization plateaus appear in a wide range of models on chains,

Send offprint requests to:

ladders, hierarchical lattices and theoretically analysed by dynamical, transfer matrix approaches as well as by the exact diagonalization in clusters [14,15,16,17,18,19]. In this paper, we obtain the magnetization plateau in 1D diamond chain using variational mean-field like treatment, based on Gibbs-Bogoliubov inequality [20,21,22,23,24,25,26].

Entanglement [27,30] has gained renewed interest with the development of quantum information science. Entangled states constitute a valuable resource in quantum information processing [31,32] for example the predicted capabilities of quantum computers rely on entanglement. Numerous different methods of entanglement measuring have been proposed for its quantification [27]. In this paper we use concurrence [33,34] as entanglement measure of the spin-1/2 system. Geometrical frustration and thermal entanglement (concurrence) of spin-1/2 Ising-Heisenberg model on a symmetrical diamond chain was studied in [35]. In this paper we study the concurrence of spin-1/2 Heisenberg model on a distorted diamond chain as the approximation of natural mineral azurite.

This paper is organized in the following way. In section 2 the variational mean-field formalism based on the Gibbs–Bogoliubov inequality is applied to the Heisenberg model on the distorted diamond chain. In section 3 we investigate the magnetic properties of the system and compare the obtained results with the experimental data of the magnetization, specific heat and magnetic susceptibility. In section 4 the concurrence of the system is calculated. Some conclusive remarks are given in the last section.

2 Gibbs-Bogoliubov approach

We use a spin–1/2 Heisenberg model. The Hamiltonian of the Heisenberg model is

$$H = \sum_{\langle i,j \rangle} J_{i,j} \boldsymbol{S}_i \boldsymbol{S}_j - \sum_i g\mu_B \boldsymbol{B} \boldsymbol{S}_i, \tag{1}$$

where $\boldsymbol{S}_i$ are the spin–1/2 operators, $J_{i,j}$ is the exchange interaction constants connecting sites i and j, $\boldsymbol{B}$ is the value of the external magnetic field, g - the gyromagnetic ratio and μ_B - the Bohr magneton. The Hamiltonian for the distorted diamond chain can be written as

$$H = J_1 \sum_i \left[\boldsymbol{\alpha}_i - \frac{h}{2}\left(S_1^{iz} + S_4^{iz}\right) - h\left(S_2^{iz} + S_3^{iz}\right) \right], \tag{2}$$

where $h = g\mu_B B^z$ and the g is set to 2,06 [36] and

$$\begin{aligned} \boldsymbol{\alpha}_i = \boldsymbol{S}_2^i \boldsymbol{S}_3^i + \delta_m \boldsymbol{S}_1^i \boldsymbol{S}_4^i + \delta_2 (\boldsymbol{S}_1^i \boldsymbol{S}_3^i + \boldsymbol{S}_2^i \boldsymbol{S}_4^i) + \\ + \delta_3 (\boldsymbol{S}_1^i \boldsymbol{S}_2^i + \boldsymbol{S}_3^i \boldsymbol{S}_4^i). \end{aligned} \tag{3}$$

where $\delta_2 = J_1/J_2,\ \delta_3 = J_3/J_2$ and $\delta_m = J_m/J_2$. Here and further exchange parameters (J_1, J_2, J_3) and the magnetic field h are taken in Boltzmann constant scaling i.e. Boltzmann constant is set to be $k_B = 1$.

Gibbs-Bogoliubov inequality [20,21,22,23,24,25,26] states that for free energy (Helmholtz potential) of the system we have

$$F \leq F_0 + \langle H - H_0 \rangle_0 , \tag{4}$$

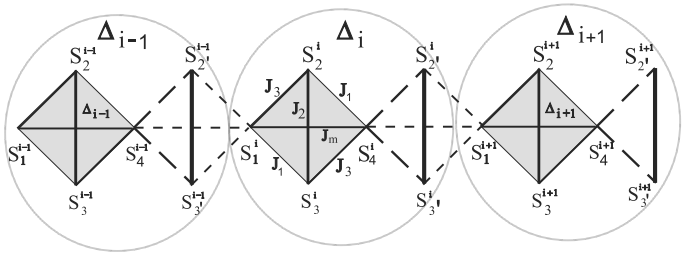

Fig. 2. Each Δ_i cluster consists of one rectangle of $\boldsymbol{S}_1^i$, $\boldsymbol{S}_2^i$, $\boldsymbol{S}_3^i$, $\boldsymbol{S}_4^i$ sites (grey rectangle) and dimer of $\boldsymbol{S}_{2'}^i$, $\boldsymbol{S}_{3'}^i$ sites (bold line).

where H is the real Hamiltonian which describes the system and H_0 is the trial one. F and F_0 are free energies corresponding to H and H_0 respectively and $\langle \ldots \rangle_0$ denotes the thermal average over the ensemble defined by H_0.

By introducing trial Hamiltonian for our model containing unknown variational parameters one can minimize right hand side of Gibbs-Bogoliubov inequality (4) and get the values of those parameters.

We introduce a trial Hamiltonian H_0 as a set of noninteracting clusters of two types in the external self-consistent field: the rectangle and the line (see Figure 2)

$$H_0 = \sum_{\Delta_i} (H_0{}^{(i)} + H_0'{}^{(i)}), \tag{5}$$

where the indexes of summation Δ_i label different noninteracting clusters and

$$\begin{aligned} H_0^{(i)} &= \lambda(\boldsymbol{\alpha}_i) - \gamma_1 S_1^{iz} - \gamma_2 S_2^{iz} - \gamma_3 S_3^{iz} - \gamma_4 S_4^{iz}, \\ H_0'^{(i)} &= \lambda'\left(\boldsymbol{S}_{2'}^i \boldsymbol{S}_{3'}^i\right) - \gamma_2' S_{2'}^{iz} - \gamma_3' S_{3'}^{iz}, \end{aligned} \tag{6}$$

where λ, λ' and γ_j, γ_j' are the variational parameters.

The real Hamiltonian (2) can be represented in the following form:

$$H = \sum_{\Delta_i} H^{(i)}, \tag{7}$$

where $H^{(i)}$ has the following form:

$$\begin{aligned} H^{(i)} = J_2 \boldsymbol{\alpha}_i - h\left(S_1^{iz} + S_2^{iz} + S_3^{iz} + S_4^{iz}\right) + J_2\left(\boldsymbol{S}_{2'}^i \boldsymbol{S}_{3'}^i\right) - \\ - h(S_{2'}^{iz} + S_{3'}^{iz}) + \frac{J_m}{2}(\boldsymbol{S}_1^i \boldsymbol{S}_4^{i-1} + \boldsymbol{S}_4^i \boldsymbol{S}_1^{i+1}) + \\ + J_1(\boldsymbol{S}_1^i \boldsymbol{S}_{3'}^{i-1} + \boldsymbol{S}_4^i \boldsymbol{S}_{2'}^i) + J_3(\boldsymbol{S}_1^i \boldsymbol{S}_{2'}^{i-1} + \boldsymbol{S}_4^i \boldsymbol{S}_{3'}^i), \end{aligned} \tag{8}$$

Gibbs-Bogoliubov inequality (4) can be rewritten now as follows:

$$\begin{aligned} f^{(i)} \leq f_0^{(i)} + (J_2 - \lambda)\langle \boldsymbol{\alpha}_i \rangle_0 + (J_2 - \lambda')\left\langle \boldsymbol{S}_{2'}^i \boldsymbol{S}_{3'}^i \right\rangle_0 + \\ + J_1(m_1 m_3' + m_4 m_2') + J_3(m_1 m_2' + m_4 m_3') + \\ + J_m(m_1 m_4) - \sum_{j=1}^{4}(h - \gamma_j) m_j - \sum_{j=2}^{3}(h - \gamma_j') m_j', \end{aligned} \tag{9}$$

where $f^{(i)} = F/N$ and $f_0^{(i)} = F_0/N$ are free energies of the one cluster (N is number of clusters) and we denote by

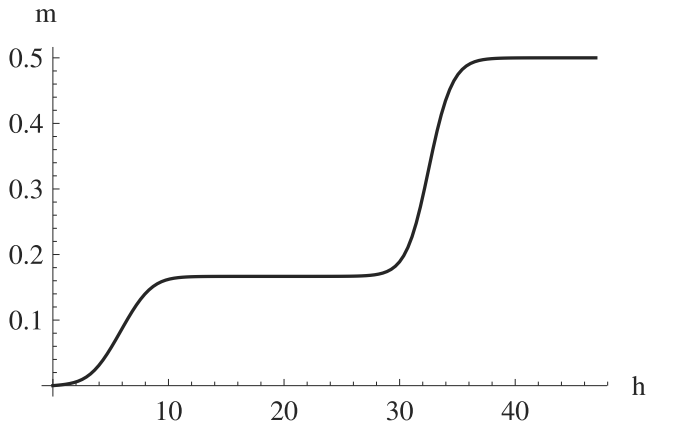

Fig. 3. Magnetization m of the cluster versus external magnetic field h (Tesla) for $J_2 = 33K$, $J_1 = 15.51\ K$, $J_3 = 6.93\ K, J_m = 4.62\ K$ at and T=1.3 K.

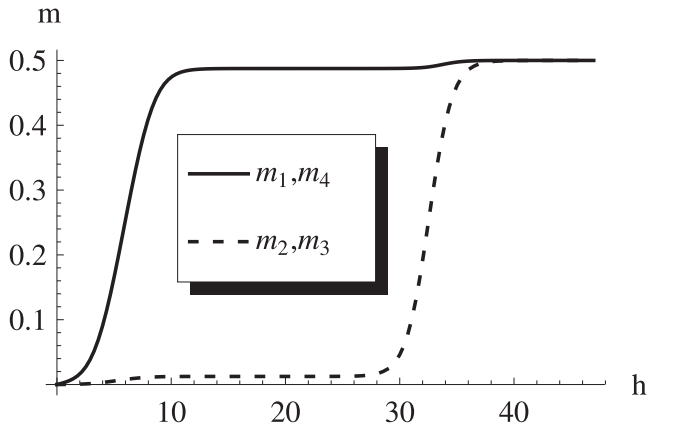

Fig. 4. Magnetizations m_1, m_2, m_3 and m_4 versus external magnetic field h (Tesla) for $J_2 = 33K$, $J_1 = 15.51\ K, J_3 = 6.93\ K, J_m = 4.6\ K$. at T=0.8 K.

$m_j \equiv \left\langle S_j^{iz} \right\rangle_0$ and $m'_{j'} \equiv \left\langle S_{j'}^{i,z} \right\rangle_0$ the magnetisations of Δ_i cluster. Here we take into account that spins of different clusters are statistically independent, i.e. $\left\langle \boldsymbol{S}_j^i \boldsymbol{S}_{k'}^{i,i\pm1} \right\rangle_0 = m_j m'_k$. For given h, J_i one must perform the minimization of r.h.s and obtain the values for γ, λ and γ', λ'. Minimizing the right hand side of (9) in order to γ_j, λ and γ'_j, λ' and using the fact, that $\dfrac{\partial f_0^{(i)}}{\partial \lambda} = \langle \boldsymbol{\alpha}_i \rangle_0$ and $\dfrac{\partial f_0^{(i)}}{\partial \gamma_j} = -m_j$ we obtain the following values for the variational parameters:

$$\begin{aligned}
\lambda &= \lambda' = J_2, \\
\gamma_2 &= \gamma_3 = h, \\
\gamma_1 &= h - J_1 m'_3 - J_3 m'_2 - J_m m_4, \\
\gamma_4 &= h - J_3 m'_3 - J_1 m'_2 - J_m m_1, \\
\gamma'_2 &= h - J_1 m_4 - J_3 m_1, \\
\gamma'_3 &= h - J_3 m_4 - J_1 m_1.
\end{aligned} \tag{10}$$

Using this values and the trial Hamiltonian one can calculate the value of any thermodynamical function of our system for the fixed h, J_i.

3 Magnetisation, specific heat and susceptibility

The results of the previous section can be used for investigation of the magnetic properties of the model. The magnetization of arbitrary site m_v of cluster Δ_i is defined as

$$m_v = \frac{Tr(S_v^{i\,z} e^{-H_0^{(i)}/T})}{Z} \tag{11}$$

where $S_v^{i\,z}$ is corresponding spin operator, $H_0^{(i)}$ is the Hamiltonian (6) and Z is the corresponding partition function of the cluster. To obtain all six magnetizations (m'_2, m'_3, $m_1, \ldots m_4$) one must insert the values of the variation parameters (10) into the equation (11) and solve the resulting system of equations for the fixed h, J_i.

$$\begin{cases}
m_1 = f_1(m'_2, m'_3, m_1, m_4) \\
\ldots \\
m_4 = f_4(m'_2, m'_3, m_1, m_4) \\
m'_2 = f'_2(m_1, m_4) \\
m'_3 = f'_3(m_1, m_4)
\end{cases} \tag{12}$$

The calculations of our paper is based on the effective diamond chain with values of coupling constants taken from [2]:

$$J_2 = 33K;\ \delta_2 = 15.51/33;\ \delta_3 = 6.93/33;\ \delta_m = 4.62/33. \tag{13}$$

The dependence of the average magnetization (for cluster)

$$m = \frac{m_1 + m_2 + m_3 + m_4 + m'_2 + m'_3}{6} \tag{14}$$

from external magnetic field, calculated from (12), is shown in Figure 3. As it can be seen from the Figure 3 the 1/3 magnetisation plateau at $T = 1.3K$ extends from 11 T to 29 T interval, while the experimental data [2,4] gave 11 T − 30 T interval.

As it mentioned above, azurite is a good candidate to exhibit $00u$ type 1/3 plateau state [10,11]. The plots in Figure 4 illustrate magnetisation versus magnetic field dependencies for different sites obtained using mean-field approach. As it can be seen from the Figure 4 dimers are essentially in the singlet state (dashed lines) whereas the single "monomer" spins are almost fully polarized in the 1/3 plateau (solid lines). The observed polarization is incompatible with a *uud* type of plateau, in which the dimer spins are strongly polarized. We find that dimer spins are about 2.5% polarized while the numerical calculation for the ideal diamond chain Heisenberg model gives 2.7% polarisation [2], while experiments give 10% [10].

The magnetic susceptibility is defined as follows:

$$\chi_0 = \left(\frac{\partial m}{\partial h} \right)_{h=0}. \tag{15}$$

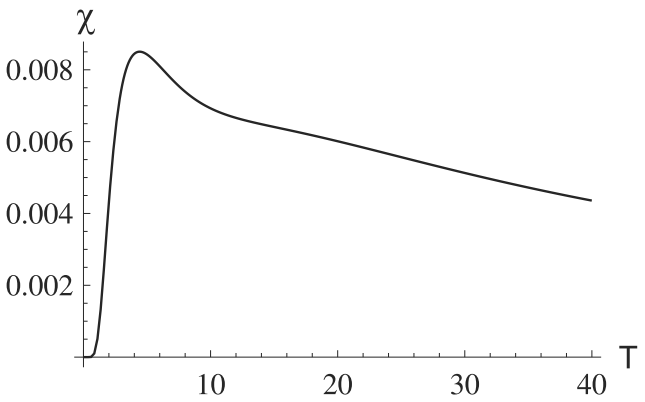

Fig. 5. Zero field magnetic susceptibility versus temperature.

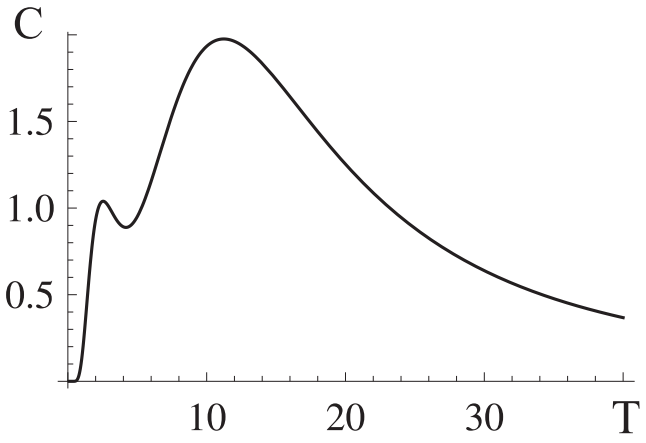

Fig. 6. Zero field specific heat versus temperature.

The magnetic susceptibility measurements of azurite performed in [4] and it was found double-peak-like structure in the magnetic susceptibility curve, namely, in the temperature dependence of the magnetic susceptibilities the sharp peak appears at $5K$ and the rounded peak is observed at $23K$. The Figure 5 shows the temperature dependence of magnetic susceptibility obtained by our calculations using (12) and (14). It has first sharp peak at $4.4K$.

Analogous to the magnetic susceptibility, we also have calculated specific heat:

$$C = -T\left(\frac{\partial^2 f_0}{\partial T^2}\right)_{h=0}. \tag{16}$$

The specific heat measurements for azurite are performed in [4] and a sharp peak is observed at $T_N = 1.8K$ signaling an ordering transition and two anomalies have been observed in the specific heat at $T = 4K$ and $T = 18K$ [4,5]. The first peak is out of reach of a one-dimensional model. Our calculations gave a low-temperature peak for $H = 0$ at $T = 3$K and the second peak at $12K$ (Figure 6). The obtained double-peak-like structure of specific heat reproduce the important features of the experimental results [2,4]. Density functional theory (DFT) [2] also gives the double-peak-like structure for the specific heat. In this paper we have reproduced the important features of the experimental results in the specific heat properties of azurite theoretically.

4 Concurrence and thermal entanglement

The mean-field like treatment transforms many- body system to the set of clusters in the effective self-consistent magnetic field. This allows to study, in particular, thermal entanglement properties of the system. The entanglement of formation [29,30] was proposed to quantify the entanglement of a bipartite system. Unfortunately the entanglement of formation extremely difficult to calculate, in general. However, in the special case of two spin 1/2 particles an analytical expression [33,34] can be obtained for the entanglement of formation of any density matrix of two spin 1/2 particles:

$$EF = H\left(\frac{(1+\sqrt{1-C^2})}{2}\right), \tag{17}$$

where

$$H(x) = -x\log_2(x) - (1-x)\log_2(1-x), \tag{18}$$

and C is the quantity called *concurrence* [33,34]. In the case of diamond chain the concurrence $C_{i,j}$ corresponding to the pair (i,j) has the following form:

$$C_{i,j} = max\{\lambda_1 - \lambda_2 - \lambda_3 - \lambda_4, 0\}, \tag{19}$$

where λ_k are the square roots of the eigenvalues (λ_1 is the maximal one) of the matrix

$$\tilde{\rho} = \rho_{ij}\cdot(\sigma_i^y \otimes \sigma_j^y)\cdot\rho_{ij}^*\cdot(\sigma_i^y \otimes \sigma_j^y), \tag{20}$$

where ρ_{ij} is the reduced density matrix for (i,j) pair. For rectangle cluster the density matrix is

$$\rho = \frac{1}{Z}\sum_{i=1}^{16} e^{-\frac{E_i}{T}}|\psi_i\rangle\langle\psi_i|, \tag{21}$$

where Z is the partition function of the rectangle and ψ_i and E_i are eigenvectors and eigenvalues of the Hamiltonian $H_0^{(i)}$ (6) respectively. The reduced density matrix of (i,j) pair ρ_{ij} can be calculated as

$$\rho_{ij} = \sum_p \left\langle \phi_p^{kl}|\rho|\phi_p^{kl}\right\rangle, \tag{22}$$

where ϕ_p^{kl} is the p-th basis vector for (k,l) remaining pair of sites of rectangle. After the calculations it has the following form

$$\rho_{ij} = \begin{pmatrix} u & 0 & 0 & 0 \\ 0 & w & y & 0 \\ 0 & y & w & 0 \\ 0 & 0 & 0 & v \end{pmatrix}, \tag{23}$$

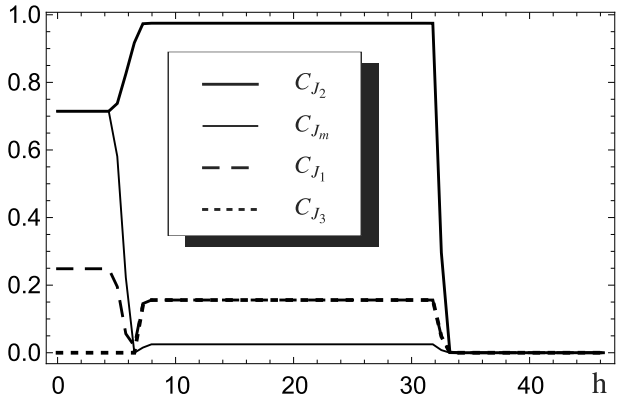

Fig. 7. The concurrences $C_{J_2}, C_{J_1}, C_{J_3}$ and C_{J_m} versus external magnetic field h (Tesla) at $T = 0.1K$ for $J_2 = 33K$, $J_1 = 15.51\ K, J_3 = 6.93\ K, J_m = 4.62\ K$.

where u, w, y and v are some functions of variables $\gamma, \lambda, \gamma', \lambda'$ and T. Using (19), (20) and (23) one can find the following expression for the concurrence $C_{i,j}$

$$C_{i,j} = 2max\{|y| - \sqrt{uv}, 0\}. \qquad (24)$$

In Figure 7 is shown the dependence of concurrences $C_{2,3} \equiv C_{J_2}$, $C_{1,2} = C_{3,4} \equiv C_{J_3}$, $C_{1,3} = C_{2,4} \equiv C_{J_1}$ and $C_{1,4} \equiv C_{J_m}$ on the magnetic field. The behavior of the concurrence can be used to analyze spin phases of azurite. As it can be seen from the Figure 7 there is three regions in magnetic field axes with different ground states. For lower value of external magnetic field the opposite spins (S_2 and S_3) in diamond cluster is highly entangled. The neighboring spins with lower coupling constant are not entangled. For higher values of h when the magnetization has a plateau the entanglement of (S_1, S_4) pair is almost zero, i. e. practically unentangled, while the (S_2, S_3) pair is almost fully entangled. The concurrence of the neighboring spins on the plateau is small, comparing to (S_2, S_3) pair, moreover the neighboring spins with lower coupling constant (J_3) are unentangled.

Now, we consider the dependence of the concurrence on temperature. Figure 8 (a) shows the temperature dependence of the concurrence for different pairs of diamond chain at small value of the magnetic field ($h = 1T$). The neighboring spins with lower coupling constant (J_3) stay unentangled with increasing temperature while the concurrence of the bigger one (J_1) decreases with temperature to $4.5K$, where the entanglement vanishes. The concurrences of J_m pair J_1 behave similar and vanish almost at the same temperature, while the dominant J_2 pair stays entangled at higher temperatures (until $28K$). Almost the same behaviour shows the temperature dependence of the concurrence for different pairs of diamond chain at plateau phase $h = 18T$ (Figure 8 (b)). The concurrences for J_m, J_3 and J_1 decrease with temperature and vanish sequential between $4K$ and $7K$ while the concurrence for J_2 pair stays entangled for the higher temperatures and vanishes at the same temperature as for small values of magnetic field ($28K$).

As it can be seen from the Figure 7 and 8b in the plateau

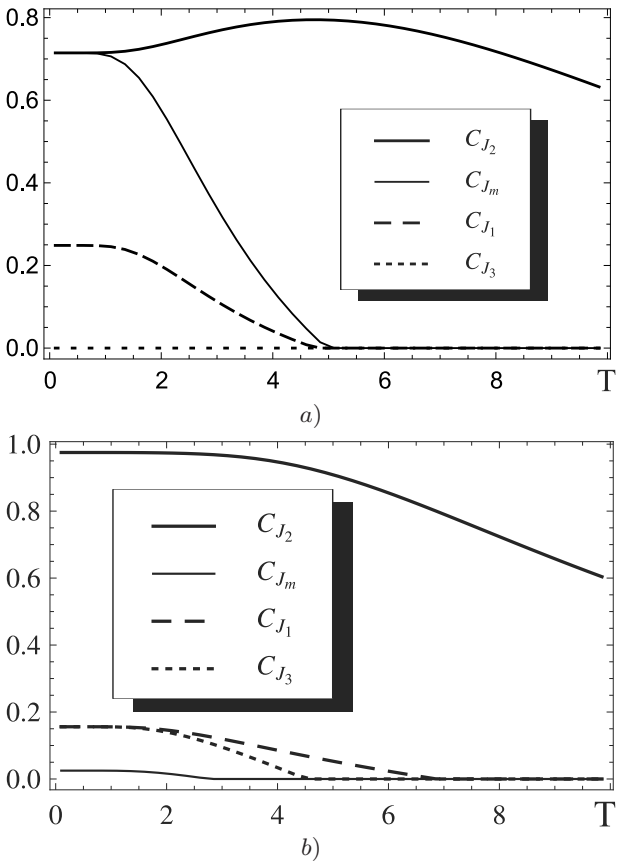

Fig. 8. The concurrences $C_{J_2}, C_{J_1}, C_{J_3}$ and C_{J_m} versus temperature for a) $h = 0T$ and b) $h = 18T$.

state dimers are almost fully entangled (lines labeled by C_{J_2} in the figures) whereas the monomer spins are weakly entangled (lines labeled by C_{J_1} and C_{J_3} in the figures). The observed entanglements is incompatible with a (uud) type of plateau, and confirm the proposed ($00u$) nature of the plateau.

Now we revert to the Figure 8 (a) to notice that comparison of the Figure 8 (a) with the Figure 6 shows that the $C(J_2)$ has a peak at nearly $T = 5K$ and it is located between two peaks of the specific heat. Roughly such a behavior can be understood as follows.

As a result of interaction between the horizontal (J_m) and vertical (J_2) dimers and also as a result of an asymmetry ($J_1 > J_3$), decreasing of the concurrences (in comparison with non-interacting case) of these dimers at zero temperature is observed. As temperature increases, energy "accumulates" in the horizontal dimer at first and in the vertical dimer later, which causes the double peak structure in the specific heat picture (see Figure 6). During the process of "energy accumulation" in the sites of the horizontal dimer (the first peak region) destruction of a quantum correlations between them takes place as a result of thermal fluctuations (so the concurrence $C(J_m)$ is decreasing, see Figure 8 (a)). And also destruction of a quantum correlations between the sites of horizontal dimer and vertical one occurs. As a consequence one can see an increasing

of $C(J_2)$ from $T = 0K$ to $T = 5K$ (without above mentioned couplings (non-interacting dimers case) $C(J_2)$ gets its maximal value equals to 1 in this region). Further temperature increasing brings destruction of the quantum correlations between the sites of the vertical dimer, which is the result of "energy accumulation" on these sites (and as a consequence - decreasing of $C(J_2)$ and increasing the specific heat to the second peak).
Varying values J_1, J_2, J_3, J_m of the coupling constants, brings to analogical picture, except the symmetric case where $J_1 = J_3$. In the symmetric case the concurrences $C(J_2) = C(J_m) = 1$ (at zero temperature) and are decreasing with the temperature and as fast as are higher the values of the $J_1 = J_3$ coupling constants. Closer is the diamond to the symmetric case, worse is the appearance of the peak structure in the $C(J_2)$ picture.

5 Conclusions

In this paper using Heisenberg model the distorted diamond chain was studied as approximation for natural material, azurite $Cu_3(CO_3)_2(OH)_2$. The magnetic properties and concurrence as a measure of pairwise thermal entanglement of the system was studied by means of variational mean-field like treatment based on Gibbs-Bogoliubov inequality. In our approach for the values of exchange parameters taken from theoretical and experimental results we have obtained the 1/3 magnetization plateau with correct critical values of magnetic field, moreover this plateau is caused by $00u$ type plateau state. We also studied the thermal entanglement properties of the distorted diamond chain and drew a parallel between them and the specific heat ones.

Acknowledgments

We would like to thank Prof. Johannes Richter for helpful discussions, comments and valuable suggestions. This work has been supported by the French-Armenian grant No. CNRS IE-017 and by the Brazilian FAPEMIG grant No. CEX - BPV - 00028-11.

References

1. A. Honecker, A. Lauchli, Phys. Rev. B **63**, 174407 (2001)
2. H. Jeschke, I. Opahle, H. Kandpal, R. Valenti, H. Das, T. Saha-Dasgupta, O. Janson, H. Rosner, A. Bruhl, B. Wolf, M. Lang, J. Richter, S. Hu, X. Wang, R. Peters, T. Pruschke, A. Honecker, Phys. Rev. Lett. **106**, 217201 (2011)
3. A. Honecker, S. Hu, R. Peters, J. Ritcher, J. Phys.: Condens. Matter **23,** 164211 (2011)
4. H. Kikuchi, Y. Fujii, M. Chiba, S. Mitsudo, T. Idehara, T. Tonegawa, K. Okamoto, T. Sakai, T. Kuwai, H. Ohta, Phys. Rev. Lett. **94**, 227201 (2005)
5. J. Kang, C. Lee, R. K. Kremer, M-H Whangbo, J. Phys.: Condens. Matter **21,** 392201 (2009)
6. B. Gu, G. Su, Phys. Rev. Lett. **97**, 089701 (2006)
7. K. C. Rule, A. U. B. Wolter, S. Sullow, D. A. Tennant, A. Bruhl, S. Kohler, B. Wolf, M. Lang, J. Schreuer, Phys. Rev. Lett. **100**, 117202 (2008)
8. H.-J. Mikeska, C. Luckmann, Phys. Rev. B **77**, 054405 (2008)
9. R. D. Spence, R.D. Ewing, Phys. Rev. **112**, 1544 (1958)
10. K. Okamoto, T. Tonegawa, M. Kaburagi, J. Phys.: Condens. Matter **15,** 5979 (2003)
11. B. Gu, G. Su, Phys. Rev. B **75**, 174437 (2007)
12. J. Schulenburg, A. Honecker, J. Schnack, J. Richter, H.-J. Schmidt, Phys. Rev. Lett. **88**, 167207 (2002)
13. O. Derzhko and J. Richter, Eur. Phys. J. B **52**, 23 (2006)
14. T. A. Arakelyan, V. R. Ohanyan, L. N. Ananikian, N. S. Ananikian, M. Roger, Phys. Rev. B **67**, 024424 (2003)
15. G. Japaridze, S. Mahdavifar, Eur. Phys. J. B **68**, 59 (2009)
16. V.V. Hovhannisyan, L.N. Ananikyan, N. S. Ananikian, Int. J. of Mod. Phys. B **21**, 3567 (2007)
17. V.V. Hovhannisyan, N.S. Ananikian, Phys. Lett. A **372**, 3363 (2008)
18. V. R. Ohanyan, N. S. Ananikian, Phys. Lett. A **307** 76 (2003)
19. N. Ananikian, L. Ananikyan, R. Artuso, H. Lazaryan, Phys. Lett. A **374,** 4084 (2010)
20. N. N. Bogoliubov J. Phys. (USSR) **11,** 23 (1947)
21. G. D. Mahan *Many-Particle Physics* (New York: Kluwer/Plenum 2000)
22. S-S Gong, G. Su Phys. Rev. A **80,** 012323 (2009)
23. M. Asoudeh, V. Karimipour Phys. Rev. A. **73,** 062109 (2006)
24. N. Canosa, J. M. Matera, R. Rossignoli, Phys. Rev. A. **76,** 022310 (2007)
25. N. S. Ananikian, L. N. Ananikyan, L. A. Chakhmakhchyan, A. N. Kocharian J. Phys. A **44,** 025001 (2011)
26. L. Ananikyan, H. Lazaryan, Journal of Contemporary Physics (Armenian Academy of Sciences) **46,** 184 (2011)
27. L. Amico, R. Fazio, A. Osterloh, V. Vedral Rev. Mod. Phys. **80,** 517 (2008)
28. R. Horodecki, P. Horodecki, M. Horodecki, K.Horodecki, Rev. Mod. Phys. **81,** 865 (2009)
29. C. H. Bennett, D. P. DiVincenzo, J. Smolin, W. K. Wootters, Phys. Rev. A **54,** 3824 (1996)
30. C. H. Bennett, G. Brassard, S. Popescu, B. Schumacher, J. Smolin, W. K. Wootters, Phys. Rev. Lett. **76,** 722 (1996)
31. C. H. Bennett, D. P. DiVincenzo, Nature **404**, 247 (2000)
32. D. Loss, D. P. DiVincenzo Phys. Rev. A **57,** 120 (1998)
33. S. Hill, W. K. Wootters Phys. Rev. Lett. **78,** 5022 (1997)
34. W. K. Wootters Phys. Rev. Lett. **80,** 2245 (1998)
35. N. Ananikian, L. Ananikyan, L. Chakhmakhchyan, O. Rojas, (e-print: cond-mat.str-el/1110.6406)
36. H. Ohta, et.al, J. Phys. Soc. Jpn. **72**, 2464 (2003)